DOI: 10.5137/1019-5149.JTN.18901-16.1
Received: 28.08.2016 / Accepted: 21.11.2016
Published Online: 12.12.2016

Original Investigation

2-Methoxyestradiol Inhibits Intracerebral Hemorrhage-Induced Angiogenesis in Rats

Hai-Tao LI[1], Hua-Jun ZHOU[2,3], Jian-Hua ZHONG[4], Tao TANG[5], Han-Jin CUI[5], Qi-Mei ZHANG[2,3], Jing-Hua ZHOU[2,3], Qiang ZHANG[2,3]

[1]China Three Gorges University, The First College of Clinical Medical Sciences, Department of Radiology, Yichang, Hubei, China
[2]China Three Gorges University, Institute of Neurology, Yichang, Hubei, China
[3]China Three Gorges University, The First College of Clinical Medical Sciences, Department of Neurology, Yichang, Hubei, China
[4]China Three Gorges University, The First College of Clinical Medical Sciences, Department of Intensive Care Unit, Yichang, Hubei, China
[5]Central South University, Institute of Integrative Medicine, Xiangya Hospital, Changsha, Hunan, China

ABSTRACT

AIM: Angiogenesis occurs after intracerebral hemorrhage (ICH). Hypoxia-inducible factor-1α (HIF-1α) is a critical regulator of angiogenesis. However, its role in the central nervous system remains controversial. 2-Methoxyestradiol (2ME2), a natural metabolite of estrogen, is known to inhibit HIF-1α. In the present study, we investigated the effect of 2ME2 in a rat model of ICH-induced angiogenesis.

MATERIAL and METHODS: Sprague-Dawley male rats (n=50) were randomly divided into 5 groups: Sham operated group; ICH; ICH+2ME2; and ICH+Vehicle groups. ICH model was induced by stereotactic injection of collagenase type VII into the right globus pallidus. 2ME2 or vehicle (10% dimethyl sulfoxide) was administered intraperitoneally 10 min after ICH. Angiogenesis and expression of HIF-1α was evaluated by immunohistochemistry, quantitative real time-reverse transcription polymerase chain reaction and western blot, respectively.

RESULTS: Proliferating cell nuclear antigen (PCNA)-labeled nuclei were detected in cerebral endothelial cells (ECs) around the hematoma. The labeling peaked at 14 days post-ICH. HIF-1α-immunoreactive microvessels with dilated outline were detected in the perihematomal tissues. The vessels extended into the clot from the surrounding tissues from day 7 onwards. HIF-1α protein levels increased, while no change was observed in HIF-1α mRNA expression after ICH. 2ME2 decreased the PCNA-labeled nuclei in cerebral ECs and down-regulated the expression of HIF-1α protein as well, while it had little effect on the mRNA expression of HIF-1α.

CONCLUSION: HIF-1α inhibitor, 2ME2, inhibited post-ICH angiogenesis by suppressing HIF-1α expression, thus exerting detrimental effects in ICH.

KEYWORDS: 2-methoxyestradiol, Intracerebral hemorrhage, Angiogenesis, Hypoxia-inducible factor-1α

INTRODUCTION

Intracerebral hemorrhage (ICH) is a life-threatening catastrophe caused by bleeding in the brain parenchyma. Although it accounts for only about 15 to 20% of all stroke events, ICH has higher mortality and disability rates as compared to other types of stroke (7,21). Despite outstanding progress in the treatment of hemorrhagic stroke in the past 10 years, little progress has been achieved in ICH treatment.

Angiogenesis, the formation of capillaries from preexisting vessels, plays a central role in a variety of physiological and pathological conditions (8). During angiogenesis, endothelial cells stimulated by angiogenic factors start to proliferate.

Corresponding author: Hua-Jun ZHOU
E-mail: zhouhuajun02@126.com

Hence, cell proliferation markers such as proliferating cell nuclear antigen (PCNA), and endothelial cell marker, von Willebrand factor (vWF), are frequently used in angiogenesis studies (15). The molecular events governing angiogenesis are complex and involve multiple families of proteins and receptors. Hypoxia-inducible factor-1α (HIF-1α) is one of the major transcriptional activators of a set of angiogenic genes such as vascular endothelial growth factor (VEGF) (28). In our previous studies, we demonstrated ICH-induced angiogenesis in rat brains, which was accompanied by up-regulation of HIF-1α (12,32).

2-Methoxyestradiol (2ME2) is an endogenous metabolite of estrogen that is known to inhibit HIF-1α in a dose-dependent manner (17). Administration of 2-ME2 has been shown to inhibit angiogenesis in both *in vivo* and *in vitro* studies (19,34). The present study was designed to clarify the effect of 2ME2 on ICH-related angiogenesis.

MATERIAL and METHODS

Animal Preparation

Adult male Sprague–Dawley (SD) rats (weight: 250-300 g each) were housed under diurnal lighting conditions. This study was carried out in strict compliance to the recommendations in the Guide for the Care and Use of Laboratory Animals of the National Institutes of Health (NIH Publication No. 85-23, revised 1996). All experiments were approved by the Institutional Animal Care and Use Committee of China Three Gorges University.

Induction of Intracerebral Hemorrhage

ICH was induced by collagenase according to the previous protocol (18). After anesthetization with chloral hydrate (400 mg/kg) via intraperitoneal injection, the animals were fixed in a prone position on a stereotactic frame (STOELTING Co., USA). Following a scalp incision, a small cranial burr was drilled near the right coronal suture, 3.2 mm lateral to the midline. Bacterial type VII collagenase (0.5 U in 2.5 μL 0.9% sterile saline, Sigma Co., USA) was slowly injected into right globus pallidus (1.4 mm posterior and 3.2 mm lateral to bregma, 5.6 mm ventral to the cortical surface) with a 5-μL Hamilton syringe for over 5 minutes. The needle was left there for another 5 minutes. The burr hole was sealed with bone wax, and the wound sutured. The animals were placed in a warm box to recover individually. In the sham group, the rats were injected with 2.5 μL 0.9% sterile saline without collagenase at the same site. During the procedure, rectal temperature was monitored and maintained at 37.5°C using a feedback controlled heating pad.

Drug Administration

2ME2 (Sigma-Aldrich Corp, MO), an HIF-1α inhibitor, was dissolved in PBS with 10% dimethyl sulfoxide (DMSO). 2ME2 (15 mg/kg, intraperitoneal injection) was administered to rats 10 minutes after induction of ICH (34). Rats in the DMSO treated group were administered the same volume of vehicle (DMSO diluted in PBS) at the same time point after induction of ICH. No treatment was administered to the ICH alone and sham-operated animals.

Neurological Evaluation

The forelimb asymmetry test was performed as described by Hua et al.(5). All rats were laid in a transparent cylinder, 20 cm in diameter and 30 cm in height. A mirror was placed near the cylinder at an angle convenient for observing the forelimb movements of the rat; and at the same time, simultaneous recording was performed by a video camera. The test lasted 10 minutes. Rat behavior was quantified by recording the number of occasions when the rat's forelimb touched the cylinder wall while it was in an orthostatic position with a balanced centre of gravity. The occasions of contact with the unimpaired (ipsilateral) forelimb were recorded as I, that with the impaired forelimb (contralateral to the collagenase injection site) as C, and movement of both forelimbs was recorded as B. The forelimb asymmetric use rate (AUR) was calculated using the following formula:

AUR = [I/(I+C+B)]-[C/(I+C+B)]. The result was evaluated by a researcher who was blinded to the experimental design.

Specimen Preparation

Randomly chosen animals from the groups were deeply anesthetized with chloral hydrate (800 mg/kg). For immunohistochemistry, animals (n=5 per time point) were transcardially perfused with 0.9% saline followed by 250 mL ice-cold 4% paraformaldehyde in 0.1 M phosphate buffer (PB, pH=7.4). The excised brains were post-fixed in the same fixative for 2 hours, and subsequently transferred to 20% and then 30% sucrose in 0.1 M PB (pH=7.4) sequentially at 4°C until sinking. Coronal sections of brain (30-μm thick) were prepared at -20°C with a cryostat (CM1900, Leica, Germany), some of which were collected in 0.01 M phosphate-buffered saline (pH=7.4) and stored at 4°C. For reverse transcription-polymerase chain reaction (RT-PCR) and western blot, rats (n=10 per time point) were transcardially perfused with 0.9% saline. The brains were immediately removed, and the tissues in striatum adjacent to the hematoma were dissected and frozen at -196°C in liquid nitrogen.

Immunohistochemistry

Under deep anesthesia with chloral hydrate (800 mg/kg), the collagenase-induced ICH animals (n=5, per time point) were randomly chosen at days 3, 7, and 14 post-operation, and were transcardially perfused with 0.9% saline followed by 250 mL ice-cold 4% paraformaldehyde in 0.1 M phosphate buffer (pH=7.4). The brains were removed and post-fixed in the same fixative for 2 hours, then transferred to 20% and 30% sucrose in 0.1 M phosphate buffer (pH=7.4), sequentially, at 4°C until sinking. Coronal sections of brain (30 μm) were prepared at -20 °C with a cryostat (CM1900, Leica Co., Germany) for immunohistochemical staining.

Proliferation of Cerebral Microvascular Endothelial Cells

Sections were pretreated to denature DNA as described below. After being immersed in 50% formamide /2× saline-sodium citrate buffer (SSC, pH=7) at 65°C for 2 hours, sections were washed with 2× SSC for 10 minutes, followed by their incubation in 2 N HCl at 37°C for 30 minutes. The nonspecific antigen was blocked by 5% bovine serum albumin (BSA,

Sigma, USA) and sections were incubated overnight with a mouse anti-PCNA (1:250, Santa Cruz Biotech, USA) at 4°C. The biotinylated anti-mouse IgG (1:200, Vector Laboratories, USA) was used for 1 hour at 37°C, and then treated with avidin-biotin-peroxidase complex (ABC) (1:100, Vector Laboratories, USA) at 37°C for 1 hour. Immunoreactivity was assessed with 3,3'- diaminobenzidine (DAB, BosterBiotech, China).

To detect the proliferated cerebral microvascular ECs, we adopted the double immunolabeling method. The procedure in the above protocol was followed after DNA denaturation, but the primary antibody was changed to rabbit anti-vWF (1:400, Chemicon International, USA), which was used to label cerebral ECs. The visualization was enhanced with ammonium nickel sulfate. The slides were observed at 40× objective magnification and the nuclei with $PCNA^+/vWF^+$ close to the hematoma were counted (four 250×250 μm areas) in randomly selected 5 sections for each animal. The data were analyzed by Motic Images Advance 3.2 image analysis software, and the results are presented as number of nuclei per mm^2 (N/mm^2). The result was evaluated by a researcher who was blinded to the experimental design.

Spatial Profile of HIF-1α after ICH

Immunohistochemical examination was performed to observe spatial profiles of HIF-1α. Briefly, sections were brought to room temperature and incubated in 3% H_2O_2 for 15 minutes. After washing 3 times in phosphate-buffered saline for 5 minutes each, nonspecific binding was blocked in 5% bovine serum albumin (Sigma Aldrich Co.) at 37°C for 1 hour. Sections were incubated with mouse anti-HIF-1α (1:200, Santa Cruz Biotech), with a biotinylated anti-mouse immunoglobulin G (1:200) for 1 hour, and then with avidin-biotin-peroxidase complex (1:100, Vector Laboratories) at 37°C for 1 hour. Immunoreactivity was visualized with diaminobenzidine (DAB, Boster Biotech Co.).

Immunofluorescence double labeling was used to detect the expression of HIF-1α in ECs. The sections were first incubated for 48 hours at 4°C with a mixture of two primary antibodies against vWF (1:200) and HIF-1α (1:100). The following secondary antibodies were used: Fluorescein isothiocyanate-conjugated donkey anti-rabbit antibody (1:50, Santa Cruz Biotechnology) for vWF detection; rhodamine-conjugated donkey anti-mouse antibody (1:100, Santa Cruz Biotechnology) for HIF-1α. These sections were scanned using a laser scanning confocal microscope (LSM-510, Zeiss, Germany).

For the negative control, 1% BSA was used instead of the primary antibody in each experiment.

Quantitative Real-Time RT-PCR

Total RNA was purified from 100 mg tissue near the hematoma in all groups using TRIZOL reagent (Invitrogen, Carlsbad, California). The integrity of total RNA was assessed on agarose gel electrophoresis; the purity and concentration were detected by a spectrophotometer (UV-1201, Shimadzu). Reverse transcription was performed on 2 μg of total RNA using 1 μg/μL oligo (dT) 18 (1 μL), 10 mM dNTP Mix (2 μL), RNase inhibitor (1 μL) and 200 U/μL M-Mulv-Reverse Transcriptase (1 μL) at 70°C for 5 minutes, at 37°C for 5 minutes, 42°C for 60 minutes and 70°C for 10 minutes following the manufacturer's instructions (Fermentas, CA, USA). cDNA was stored at -20°C. PCR amplification was performed using SYBR Premix ExTaq™ PCR kit (4 μL of 1:2 cDNA dilution was used, Takara Biotechnology, Japan) in a LightCycler Real-Time Detection System (Roche Diagnostics Limited, Germany). The following thermocycling protocol was used: 10 seconds at 95°C; 30 cycles of 5 seconds at 95°C, 20 seconds at 52°C , and 10 seconds at 72°C; and a melting curve at 60°C. Primers for HIF-1α and β-actin were designed with Primer Premier 5.0 software for rat (PRIMER Biosoft International, CA, USA) as follows:

HIF-1α, sense 5 were designed with Primer Premier 5.0 software for rat (PRIMER Biosoft Inter β-actin, sense5'-CGTTGACATCCGTAAAGAC -3' and antisense 5'-TGGAAGGTGGACAGTGAG -3'.

Melting curves of all samples were prepared as controls to test specificity. All gene expression data were calculated by $2^{-\Delta\Delta CT}$, which indicates an n-fold change in gene expression relative to the sham control sample (11).

Western Blot

Protein was extracted from the striatal tissues adjacent to the hematoma. Western blot analysis was performed (23). Briefly, 50-μg proteins were separated by sodium dodecyl sulfate polyacrylamide gel electrophoresis and transferred to a Hybond-C pure nitrocellulose membrane (Amersham). Monoclonal mouse antibodies for HIF-1α (1:100) and β-actin (1:200, Santa Cruz Biotech, CA, USA) were used. Quantitative densitometric analysis of Western blots was performed with a computerized digital image analysis system.

Statistical Analysis

All data are expressed as mean ± standard deviation (SD). One-way Analysis of Variance (ANOVA) was used to compare between-group the differences. P value less than 0.05 was considered statistically significant.

■ RESULTS

Neurological Evaluation

The AUR for all the groups are shown in Figure 1A,B. No neurological deficit was observed in the sham operated rats. After ICH, the rats were observed for neurological deficit: the AUR gradually decreased as the observation time progressed (Figure 1A, $p<0.01$). After 2ME2 treatment, the AUR values notably increased from 7 days as compared to those in the ICH+DMSO groups (Figure 1B, $p<0.05$).

Angiogenesis Following ICH

After ICH, some PCNA-positive cells in von Willebrand factor (vWF) - immunoreactive dilated vessels were detected around the clot (Figure 2A,B), and the $PCNA^+/vWF^+$ nuclei increased notably over time (Figure 2C, $p<0.05$). After 2ME2 treatment, the number of $PCNA^+/vWF^+$ nuclei was decreased significantly

as compared to that in the ICH+DMSO groups (Figure 2D, p<0.05).

Spatial Distribution of HIF-1α after ICH

The immunohistochemical staining of HIF-1α is shown in Figure 3. In the sham-operated animals, few HIF-1α-positive vessels were observed (Figure 3A). However, some HIF-1α-positive dilated vessels were detected mainly in the perihematomal tissue, and these positive vessels extended into the clot from 7 days after ICH (Figure 3B). Furthermore, immunofluorescent double labeling confirmed that HIF-1α was localized to vWF^+ vessels around the hematoma (Figure 3C-E).

HIF-1α mRNA and Protein Analysis

No signals of HIF-1α mRNA and protein were detected in the sham-operated rats. After ICH induction, the HIF-1α protein levels increased markedly at 3 days, and then declined. However, HIF-1α mRNA levels were unchanged. The levels of HIF-1 protein in the 2ME2+ICH group were significantly lower than those in the ICH+DMSO groups (p<0.05). However, 2ME2 had little effect on the expression of HIF-1α mRNA (Figure 4A,B).

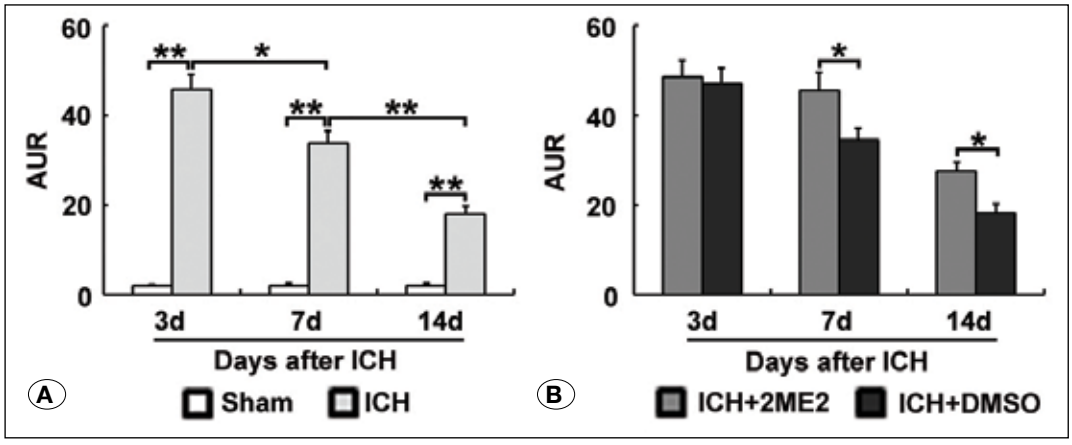

Figure 1: Neurological evaluation.
Behavioral tests were implemented in rats after ICH or sham operation. The ICH group was distinctly worse impaired as compared to the sham group at the corresponding time points. The AUR values of the ICH+2ME2 group were significantly higher than that of ICH+DMSO group from 7 days post ICH. (*p<0.05, **p<0.01, n=10).

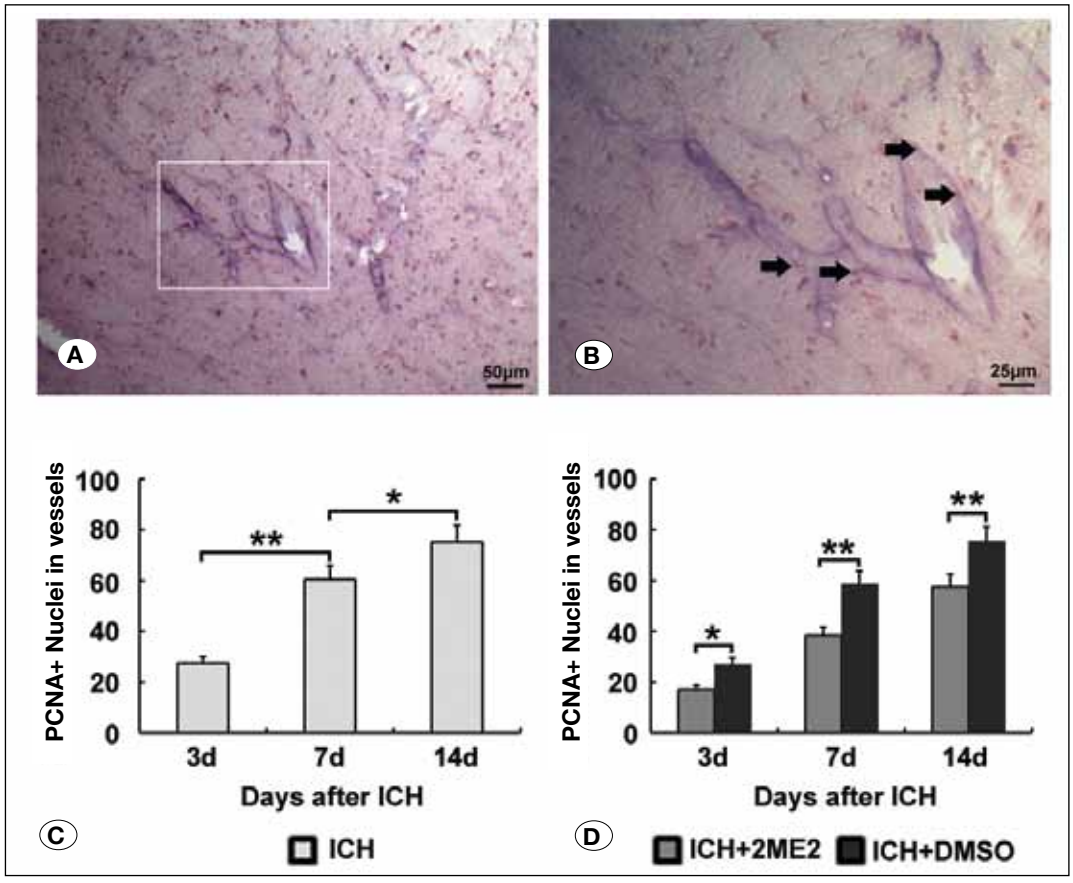

Figure 2: Proliferated cerebral endothelial cells after ICH.
Post-ICH induction, some PCNA-positive cells (brown, arrow) in vWF-immunoreactive dilated vessels (blue) were detected around the hematoma **(A, B)**; the $PCNA^+/vWF^+$ nuclei increased up till 14 days **(C)**; 2ME2 markedly increased the expression levels of PCNA-positive cells in the vWF-immunoreactive vessels **(D)**.
* p<0.05, ** P<0.01. Scale bar, 50 μm for panel A, 25 μm for panel B.

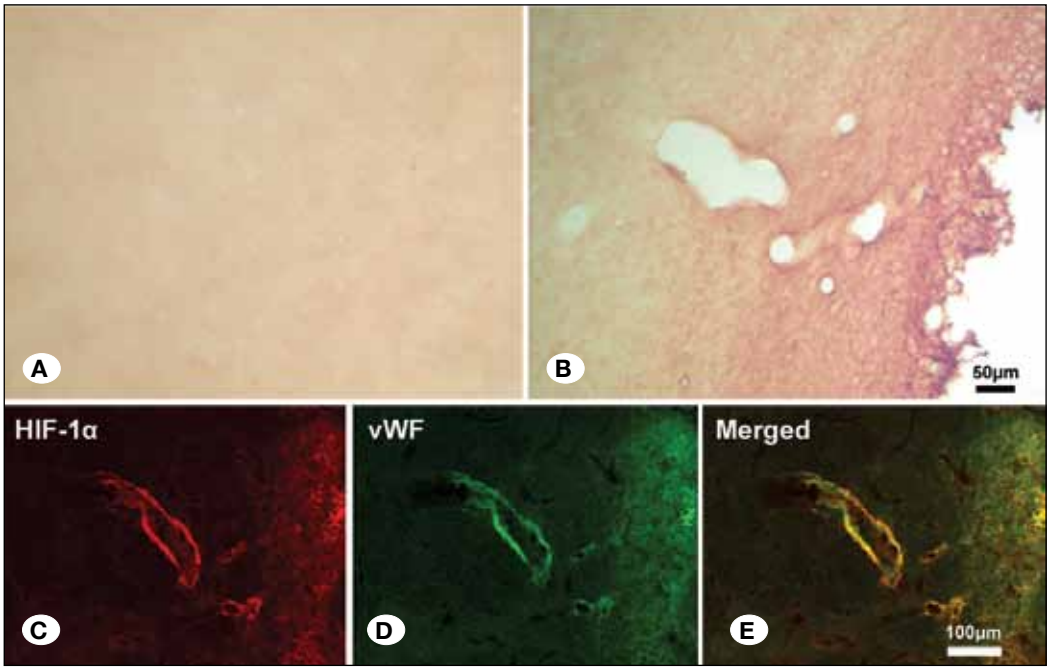

Figure 3: Immunohistochemical examination for detection of HIF-1α.
HIF-1α positive signals were hardly observed in the brains of sham-operated animals **(A)**. After ICH, HIF-1α immunoreactive microvessels with the dilated outline were detected in the perihematomal tissues **(B)**. Immunofluorescent double labeling showed that HIF-1α (red) was localized in vWF+ (green) vessels after ICH **(C-E)**. Scale bar, 50 μm for panels **A-B**, 100 μm for panels **C-E**.

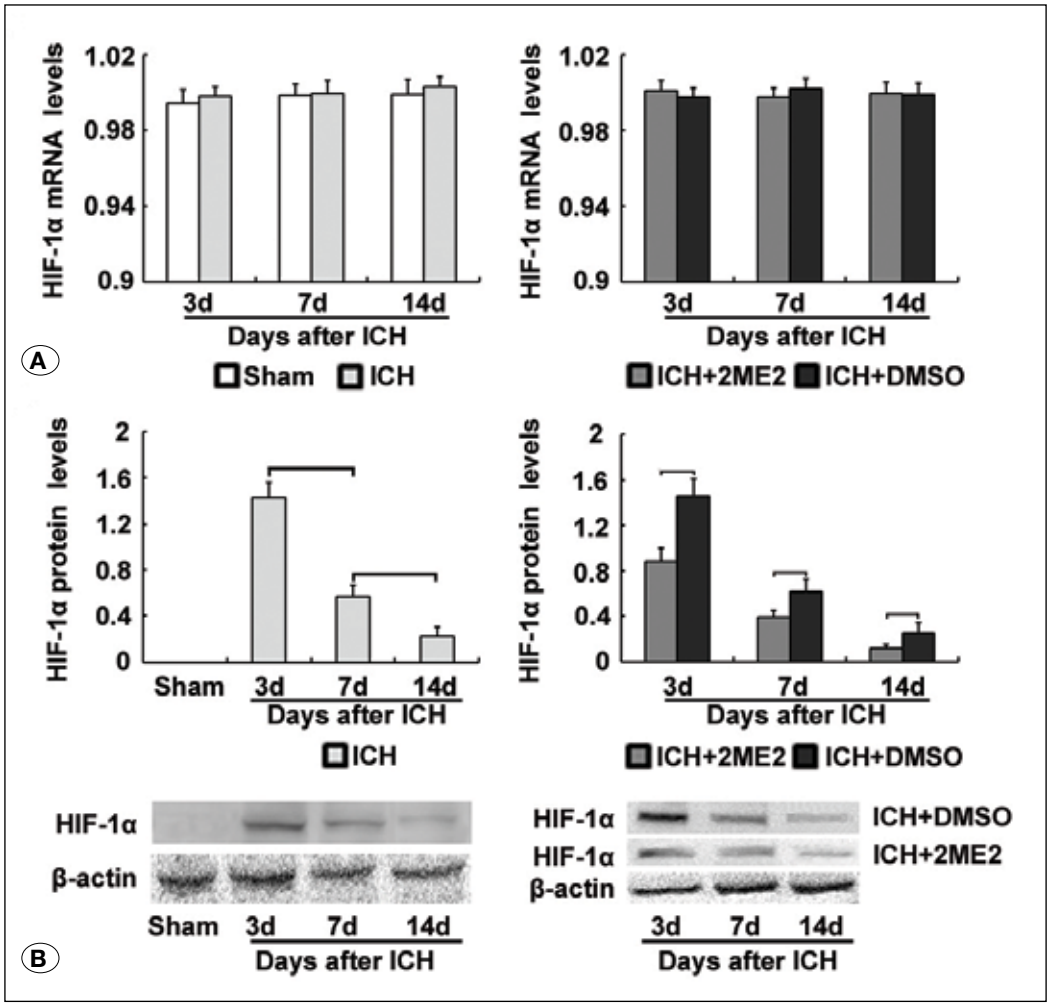

Figure 4: Quantitative analysis of HIF-1α mRNA and protein after ICH.
After induction of ICH, HIF-1α mRNA levels did not change at any time-point in all groups **(A)**, while the HIF-1α protein level increased at 3 days followed by a decline. 2ME2 strikingly down-regulated the HIF-1α protein expression **(B)**. *p<0.05, **P<0.01.

DISCUSSION

In the present study, we demonstrated detrimental effects of 2ME against hemorrhagic injury in rats. After ICH, PCNA-positive cells were detected in the vWF- immunoreactive dilated vessels around the clot. Further, a notable increase in the $PCNA^+/vWF^+$ nuclei was observed accompanied by enhanced expression of HIF-1α. 2ME2 decreased the number of $PCNA^+/vWF^+$ nuclei by down-regulating the expression of HIF-1α. The findings indicate that HIF-1α plays a critical role in ICH-induced angiogenesis, that 2ME2 is a potent inhibitor of angiogenesis.

HIF-1α is a helix-loop-helix transcription factor that is ubiquitously expressed in mammalian cells. Under normoxic conditions, HIF-1α is rapidly degraded by proteasome (6,22). Hence, no HIF-1α signal could be detected in the sham control group. Other studies have also demonstrated a central role of HIF-1α in angiogenesis (25,33). In our previous study, we found abundant HIF-1α immunoreactive microvessels in ECs in the vicinity of the clot (12,32). The spatiotemporal profile is also consistent with post-ICH angiogenesis. Therefore, it is tempting to suppose that HIF-1α may be a crucial mediator for ICH-induced angiogenesis.

To confirm this presumption, 2ME2, a HIF-1α inhibitor, was used in this study. 2ME2, a natural metabolite of estradiol, has been shown to inhibit tumor growth and angiogenesis by inducing dysregulation of HIF-1α (13,14). At a dose of 16 mg/kg, 2ME2 can effectively inhibit the expression of HIF-1α (31,34). 2ME2 not only depolymerizes microtubules and blocks nuclear accumulation of HIF-1α and HIF-transcriptional activity, but also downregulates HIF-1α at the posttranscriptional level (1,14). Consistent with other studies, the present study showed that 2ME2 could inhibit ICH-induced angiogenesis by downregulating HIF-1α at protein levels and without altering HIF-1α transcriptional level.

The role of HIF-1α in central nervous system remains controversial. Inhibition of HIF-1α was shown to have a neuroprotective effect after cerebral ischemia, which was associated with preservation of blood brain barrier integrity (9,30), amelioration of brain edema (3,16), and prevention of neuronal death (2). Moreover, Yan et al. reported that 2-ME2 reduced cerebral vasospasm after subarachnoid hemorrhage by inhibiting HIF-1α (24). Additionally, normobaric oxygen therapy was shown to reduce neurological deficits by suppressing HIF-1α expression in the perihematoma (26). However, some conflicting findings have also been reported on the exact role of HIF-1α after cerebral ischemia (19,20,29,31) and ICH (10,27). In the present study, Inhibition of HIF-1α by 2ME2 not only reduced post-ICH angiogenesis but also delayed functional recovery. The discrepancy in findings may be attributable to different time-frame, different stroke models or different inhibitors of HIF-1α used in these studies. Intriguingly, inhibition of HIF-1α by 2ME2 aggravated ICH-induced neurological deficits from 7 days, which indicated that 2ME2 exerted detrimental effects at the late stage of ICH. Since HIF-1α is also involved in neurogenesis after stroke (4), the effects of 2ME2 on ICH-related neurogenesis requires further investigation.

CONCLUSION

We demonstrate for the first time that the HIF-1α inhibitor, 2ME2 impaired post-ICH angiogenesis and functional recovery. These findings indicate that HIF-1α may have a protective effect against ICH-induced damage. However, further investigations are essential to elucidate the precise mechanisms of HIF-1α action before proposing it as a neuroprotective target for the treatment of ICH.

ACKNOWLEDGMENT

This study was supported by grants from the National Natural Science Foundation of China (Grant Nos. 30400581, 30873221, 81173175, and 81202625), the Project for New Century Excellent Talents (NCET-11-0522), the Hunan Provincial Natural Science Foundation (Grant Nos. 07JJ5007 and 10JJ2023), and the Key Laboratory of cardiovascular and cerebrovascular diseases translational medicine (Three Gorges University, 2016xnxg202).

REFERENCES

1. Chen C, Hu Q, Yan J, Lei J, Qin L, Shi X, Luan L, Yang L, Wang K, Han J, Nanda A, Zhou C: Multiple effects of 2ME2 and D609 on the cortical expression of HIF-1alpha and apoptotic genes in a middle cerebral artery occlusion-induced focal ischemia rat model. J Neurochem 102:1831-1841, 2007
2. Cheng YL, Park JS, Manzanero S, Choi Y, Baik SH, Okun E, Gelderblom M, Fann DY, Magnus T, Launikonis BS, Mattson MP, Sobey CG, Jo DG, Arumugam TV: Evidence that collaboration between HIF-1alpha and Notch-1 promotes neuronal cell death in ischemic stroke. Neurobiol Dis 62:286-295, 2014
3. Higashida T, Peng C, Li J, Dornbos D 3rd, Teng K, Li X, Kinni H, Guthikonda M, Ding Y: Hypoxia-inducible factor-1alpha contributes to brain edema after stroke by regulating aquaporins and glycerol distribution in brain. Curr Neurovasc Res 8:44-51, 2011
4. Hu Q, Liang X, Chen D, Chen Y, Doycheva D, Tang J, Tang J, Zhang JH: Delayed hyperbaric oxygen therapy promotes neurogenesis through reactive oxygen species/hypoxia-inducible factor-1alpha/beta-catenin pathway in middle cerebral artery occlusion rats. Stroke 45:1807-1814, 2014
5. Hua Y, Schallert T, Keep RF, Wu J, Hoff JT, Xi G: Behavioral tests after intracerebral hemorrhage in the rat. Stroke 33: 2478-2484, 2002
6. Jiang BH, Rue E, Wang GL, Roe R, Semenza GL: Dimerization, DNA binding, and transactivation properties of hypoxia-inducible factor 1. J Biol Chem 271:17771-17778, 1996
7. Jolink WM, Klijn CJ, Brouwers PJ, Kappelle LJ, Vaartjes I: Time trends in incidence, case fatality, and mortality of intracerebral hemorrhage. Neurology 85:1318-1324, 2015
8. Lancerotto L, Orgill DP: Mechanoregulation of angiogenesis in wound healing. Adv Wound Care (New Rochelle) 3: 626-634, 2014
9. Lee JH, Cui HS, Shin SK, Kim JM, Kim SY, Lee JE, Koo BN: Effect of propofol post-treatment on blood-brain barrier integrity and cerebral edema after transient cerebral ischemia in rats. Neurochem Res 38: 2276-2286, 2013

10. Lei C, Lin S, Zhang C, Tao W, Dong W, Hao Z, Liu M, Wu B: Effects of high-mobility group box1 on cerebral angiogenesis and neurogenesis after intracerebral hemorrhage. Neuroscience 229:12-19, 2013
11. Livak KJ, Schmittgen TD: Analysis of relative gene expression data using real-time quantitative PCR and the 2(-Delta Delta C(T)) method. Methods 25:402-408, 2001
12. Luo JK, Zhou HJ, Wu J, Tang T, Liang QH: Electroacupuncture at Zusanli (ST36) accelerates intracerebral hemorrhage-induced angiogenesis in rats. Chin J Integr Med 19: 367-373, 2013
13. Ma L, Li G, Zhu H, Dong X, Zhao D, Jiang X, Li J, Qiao H, Ni S, Sun X: 2-Methoxyestradiol synergizes with sorafenib to suppress hepatocellular carcinoma by simultaneously dysregulating hypoxia-inducible factor-1 and -2. Cancer Lett 355: 96-105, 2014
14. Mabjeesh NJ, Escuin D, LaVallee TM, Pribluda VS, Swartz GM, Johnson MS, Willard MT, Zhong H, Simons JW, Giannakakou P: 2ME2 inhibits tumor growth and angiogenesis by disrupting microtubules and dysregulating HIF. Cancer Cell 3: 363-375, 2003
15. Peng ZR, Yang AL, Yang QD: The effect of hyperbaric oxygen on intracephalic angiogenesis in rats with intracerebral hemorrhage. J Neurol Sci 342:114-123, 2014
16. Reischl S, Li L, Walkinshaw G, Flippin LA, Marti HH, Kunze R: Inhibition of HIF prolyl-4-hydroxylases by FG-4497 reduces brain tissue injury and edema formation during ischemic stroke. PloS one 9: e84767, 2014
17. Ricker JL, Chen Z, Yang XP, Pribluda VS, Swartz GM, Van Waes C: 2-methoxyestradiol inhibits hypoxia-inducible factor 1alpha, tumor growth, and angiogenesis and augments paclitaxel efficacy in head and neck squamous cell carcinoma. Clin Cancer Res 10: 8665-8673, 2004
18. Rosenberg GA, Mun-Bryce S, Wesley M, Kornfeld M: Collagenase-induced intracerebral hemorrhage in rats. Stroke 21:801-807, 1990
19. Salih SM, Kapur A, Albayrak S, Salama SA, Magness RR: Pregnancy ameliorates the inhibitory effects of 2-methoxyestradiol on angiogenesis in primary sheep uterine endothelial cells. Reprod Sci 18:858-867, 2011
20. Sun Y, He W, Geng L: Neuroprotective mechanism of HIF-1alpha overexpression in the early stage of acute cerebral infarction in rats. Exp Ther Med 12: 391-395, 2016
21. Tsai CF, Thomas B, Sudlow CL: Epidemiology of stroke and its subtypes in Chinese vs white populations: A systematic review. Neurology 81:264-272, 2013
22. Wang GL, Jiang BH, Rue EA, Semenza GL: Hypoxia-inducible factor 1 is a basic-helix-loop-helix-PAS heterodimer regulated by cellular O_2 tension. Proc Natl Acad Sci USA 92:5510-5514, 1995
23. Xi G, Keep RF, Hua Y, Xiang J, Hoff JT: Attenuation of thrombin-induced brain edema by cerebral thrombin preconditioning. Stroke 30:1247-1255, 1999
24. Yan J, Chen C, Lei J, Yang L, Wang K, Liu J, Zhou C: 2-methoxyestradiol reduces cerebral vasospasm after 48 hours of experimental subarachnoid hemorrhage in rats. Exp Neurol 202:348-356, 2006
25. Yang Y, Sun M, Wang L, Jiao B: HIFs, angiogenesis, and cancer. J Cell Biochem 114: 967-974, 2013
26. You P, Lin M, Li K, Ye X, Zheng J: Normobaric oxygen therapy inhibits HIF-1alpha and VEGF expression in perihematoma and reduces neurological function defects. Neuroreport 27: 329-336, 2016
27. Yu Z, Chen LF, Tang L, Hu CL: Effects of recombinant adenovirus-mediated hypoxia-inducible factor-1alpha gene on proliferation and differentiation of endogenous neural stem cells in rats following intracerebral hemorrhage. Asian Pac J Trop Med 6: 762-767, 2013
28. Zhang K, Han ES, Dellinger TH, Lu J, Nam S, Anderson RA, Yim JH, Wen W: Cinnamon extract reduces VEGF expression via suppressing HIF-1alpha gene expression and inhibits tumor growth in mice. Mol Carcinog 2016 Jun 2 (Epub ahead of print)
29. Zhang P, Li W, Li L, Wang N, Li X, Gao M, Zheng J, Lei S, Chen X, Lu H, Liu Y: Treatment with edaravone attenuates ischemic brain injury and inhibits neurogenesis in the subventricular zone of adult rats after focal cerebral ischemia and reperfusion injury. Neuroscience 201:297-306, 2012
30. Zhang Z, Yan J, Shi H: Role of hypoxia inducible factor 1 in hyperglycemia-exacerbated blood-brain barrier disruption in ischemic stroke. Neurobiol Dis 95: 82-92, 2016
31. Zheng J, Zhang P, Li X, Lei S, Li W, He X, Zhang J, Wang N, Qi C, Chen X, Lu H, Liu Y: Post-stroke estradiol treatment enhances neurogenesis in the subventricular zone of rats after permanent focal cerebral ischemia. Neuroscience 231:82-90, 2013
32. Zhou HJ, Tang T, Cui HJ, Yang AL, Luo JK, Lin Y, Yang QD, Li XQ: Thrombin-triggered angiogenesis in rat brains following experimental intracerebral hemorrhage. J Neurosurg 117:920-928, 2012
33. Zimna A, Kurpisz M: Hypoxia-inducible factor-1 in physiological and pathophysiological angiogenesis: Applications and therapies. Biomed Res Int 2015:549412, 2015
34. Zou X, Zhou L, Zhu W, Mao Y, Chen L: Effectiveness of 2-methoxyestradiol in alleviating angiogenesis induced by intracranial venous hypertension. J Neurosurg 11:1-8, 2015